

Magnetic susceptibility of $\text{Cs}_2\text{CrCl}_5 \cdot 4\text{H}_2\text{O}$: Interplay of exchange and crystal-field effects

Richard L. Carlin and Ramon Burriel

Department of Chemistry, University of Illinois at Chicago, Chicago, Illinois 60680

(Received 4 June 1982)

The single-crystal susceptibilities of $\text{Cs}_2\text{CrCl}_5 \cdot 4\text{H}_2\text{O}$ are reported over the temperature interval 40 mK–4.2 K. Long-range magnetic ordering is found to occur at 0.185 ± 0.005 K. Successful data analysis has been carried out in terms of a spin $S = \frac{3}{2}$ Heisenberg linear-chain antiferromagnet with crystal-field and exchange energies of comparable magnitude; the resulting parameters are $g_z = 1.98$, $g_1 = 1.95$, $D/k_B = -0.16$ K, $E/k_B = -0.05$ K, and $J/k_B = -0.045$ K.

INTRODUCTION

Chromium(III), a d^3 ion, forms a large number of coordination compounds. All of them are of six-coordinate, octahedral stereochemistry, with spin $S = \frac{3}{2}$. With the important exception of the alums, in which dipole-dipole interactions predominate, few chromium compounds have been studied at low temperatures. Our interest in chromium systems lies with the fact that the 4A_2 ground state is susceptible to zero-field splitting effects which are typically smaller than 0.5 K; tetrahedral cobalt(II) also exhibits the same ground state, but it is typically split into two doublets which are separated by 10–15 K.¹ Therefore, only the lowest doublet is populated at low temperatures, and cobalt has an effective spin $S = \frac{1}{2}$. By contrast, zero-field splittings with chromium may be comparable to exchange interactions and therefore provides a more challenging problem for the analysis of data.² The situation is similar to that with nickel(II), which is famous for having its magnetic ordering phenomena determined by its crystal-field splittings.^{3–5} Copper(II), an $S = \frac{1}{2}$ ion, has been well studied but cannot exhibit zero-field splitting; manganese(II), an $S = \frac{5}{2}$ ion, has also been well studied, but crystal-field splittings are generally much smaller than exchange energy. One exception to this rule is provided by $[\text{Mn}(\text{C}_5\text{H}_5\text{NO})_6](\text{BF}_4)_2$.⁶ An extensive series of $S = \frac{5}{2}$ antiferromagnets of formula $A_2\text{FeX}_5 \cdot \text{H}_2\text{O}$ has recently been studied,⁷ and again the crystal-field splittings are considerably smaller than the exchange energies.

We report here magnetic susceptibility measurements on the compound $\text{Cs}_2\text{CrCl}_5 \cdot 4\text{H}_2\text{O}$, which seems to be a good example of the situation

described above, that of having crystal-field and exchange energies of comparable magnitude.

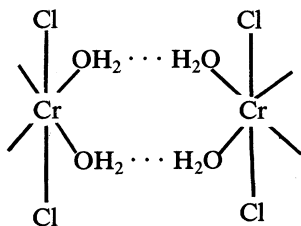
EXPERIMENTAL

Single crystals were obtained according to the literature⁸ by mixing CsCl and $\text{CrCl}_3 \cdot 6\text{H}_2\text{O}$ in 2M HCl. Crystals were oriented for magnetic measurements by x-ray precession methods. Susceptibilities were measured by an ac mutual inductance procedure as described earlier.⁹

CRYSTAL STRUCTURE

The monoclinic compound belongs⁸ to the space group $C2/m$ with $a = 17.604$ Å, $b = 6.140$ Å, $c = 6.979$ Å, $\beta = 106.04^\circ$, and $Z = 2$. The compound contains *trans*- $[\text{CrCl}_2(\text{H}_2\text{O})_4]^+$ groups of almost perfect D_{4h} symmetry. The Cr-Cl distance is 2.302 Å and there is substantial hydrogen bonding in the lattice. The remaining chloride ions are not coordinated to the metal. Along the a axis, the chromium ions are separated by 17.604 Å, and this long distance precludes any superexchange interaction between these chromium ions. There is another chromium atom in the ab plane, at the center of a rectangle of chromium atoms which are situated at the vertices of the unit cell, but since it is 9.322 Å from its nearest chromium neighbor, and since there is not a good superexchange path which connects it with its neighbors, one does not expect it to contribute strongly to the exchange interaction. In other words, superexchange interaction along the a axis is expected to be weak, and one can therefore anticipate the appearance of lower-dimensional magnetic effects.

This idea is reinforced by an examination of the most likely superexchange paths in the remaining directions. The crystal structure contains chains along the b axis of the kind



which form a plane perpendicular to the ac plane and which lies 38° from the bc plane towards the a axis. Two chlorides lie above this unit and two are below, the four chlorides in a plane perpendicular to the plane illustrated above. Along the c axis, then, the metals are separated by 6.979 \AA ; there are chloride ions on the perpendicular bisector of the metal-metal vector. The best superexchange path is provided along the b axis, where the chromiums are separated by 6.140 \AA . Two water molecules in *cis* positions on neighboring metals face each other, as described above, with an oxygen-oxygen separation of 3.411 \AA ; above and below the plane formed by these hydrogen-bonded water molecules lie four uncoordinated chloride ions. These latter strengthen the superexchange interaction in this dimension and indeed suggest the presence of a (weak) magnetic linear chain interaction along the b axis. In the discussion below, we associate the x direction with the b axis, which by symmetry is necessarily a principal

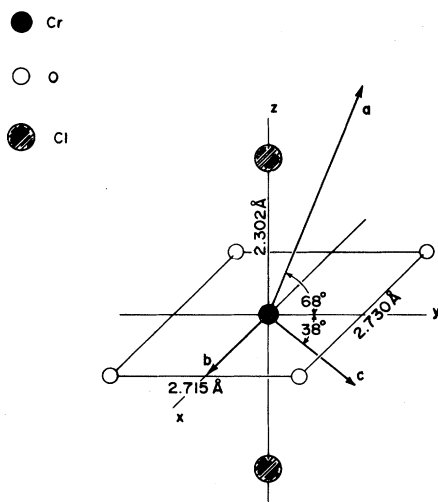


FIG. 1. Octahedral environment of the chromium ion with distances and relative orientation of the crystal axes.

axis of the susceptibility tensor. Then, the y axis must be a perpendicular axis, and we retain the notation of z for the third spacial axis. The z axis lies 22° from the a axis in the ac plane. This local coordinate system is illustrated in Fig. 1.

THEORETICAL BACKGROUND

The crystal-field theory of chromium(III) is well known. The ground state in an octahedral environment is 4A_2 , which is well separated from all the higher-energy states. The degeneracy of this state may be resolved into its $m_s = |\pm \frac{1}{2}\rangle$ and $|\pm \frac{3}{2}\rangle$ components by the presence of a small axial crystal-line field. The separation is denoted by $2D$ where D has both sign and magnitude. The susceptibilities are easily calculated in this case.²

When a rhombic distortion is added, the zero-field splitting becomes $\delta = 2(D^2 + 3E^2)^{1/2}$. The Hamiltonian we use is

$$\mathcal{H} = g\mu_B \vec{H} \cdot \vec{S} + D[S_z^2 - (\frac{1}{3})S(S+1)] + E(S_x^2 - S_y^2).$$

The solutions for the energy levels have been written down explicitly¹⁰ and need not be repeated here. The general form for the susceptibility¹¹ is

$$\chi_i = \frac{Ng_i^2 \mu_B^2}{k_B T} \left[\left(\frac{4A_i^2}{\delta^2} + \frac{1}{4} \right) + \left(\frac{24B_i^2}{X\delta^2} - \frac{2A_i}{\delta} \right) \left(\frac{1-e^{-X}}{1+e^{-X}} \right) \right], \quad (1)$$

where $X = \delta/k_B T$, $i = x, y, z$, $A_x = -\frac{1}{2}(D-3E)$, $A_y = -\frac{1}{2}(D+3E)$, $A_z = D$; $B_x = +\frac{1}{2}(D+E)$, $B_y = \frac{1}{2}(D-E)$, and $B_z = E$. Exchange effects may be accounted for in the usual molecular field approximation^{4,12} as

$$\chi'_i = \chi_i [1 - (2zJ/Ng_i^2 \mu_B^2) \chi_i]^{-1}. \quad (2)$$

In the linear approximation when $|E|$, $|D|$, and $|J|$ are all much smaller than $k_B T$, we find

$$\chi'_b = \frac{Ng_b^2 \mu_B^2}{3k_B T} \left[\frac{15}{4} + \left(\frac{75}{8} \frac{zJ}{k_B} + \frac{3}{2} \frac{(D-3E)}{k_B} \right) \left(\frac{1}{T} \right) \right], \quad (3)$$

$$\chi'_y = \frac{Ng_y^2\mu_B^2}{3k_B T} \left[\frac{15}{4} + \left(\frac{75}{8} \frac{zJ}{k_B} + \frac{3}{2} \frac{(D+3E)}{k_B} \right) \left(\frac{1}{T} \right) \right], \quad (4)$$

$$\chi'_z = \frac{Ng_z^2\mu_B^2}{3k_B T} \left[\frac{15}{4} + \left(\frac{75}{8} \frac{zJ}{k_B} - \frac{3D}{k_B} \right) \left(\frac{1}{T} \right) \right]. \quad (5)$$

Note that plots of $\chi'_i T$ vs $1/T$ should be linear at high temperatures. Equations (3)–(5) contain six unknowns, but the slope and intercept of each of these independent equations provides a total of six relationships, which thereby provides enough information for a simultaneous solution.

RESULTS

The zero-field magnetic susceptibility of $\text{Cs}_2\text{CrCl}_5 \cdot 4\text{H}_2\text{O}$ was measured at a constant temperature of 4.2 K as a function of angle in the ac plane. The rotation diagram is illustrated in Fig. 2. A small but measurable anisotropy is evident. The data may be fitted by the usual relation

$$\chi = \chi_{\parallel} \cos^2 \theta + \chi_{\perp} \sin^2 \theta, \quad (6)$$

where $\chi_{\parallel} \equiv \chi_z = 0.420$ emu/mol and $\chi_{\perp} \equiv \chi_y = 0.393$ emu/mol. These data define the two principal axes in the ac plane as suggested above.

The experimental data are presented in Fig. 3. It may be seen that the susceptibility in the z direction reaches a maximum at 0.27 ± 0.01 K and then drops towards zero at 0 K. Taking these measurements to indicate antiferromagnetic ordering with the z axis as the preferred axis of spin alignment, an ordering

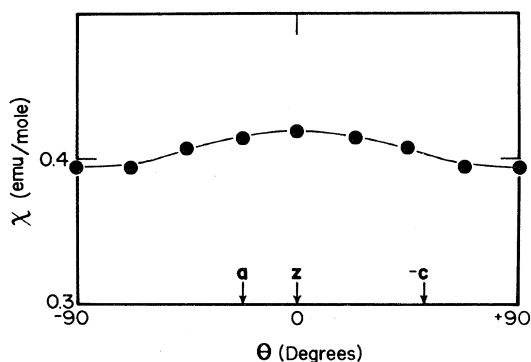


FIG. 2. Angular dependence of the zero-field susceptibilities of $\text{Cs}_2\text{CrCl}_5 \cdot 4\text{H}_2\text{O}$ in the ac plane, equivalent to the yz plane. The origin is taken at the z axis.

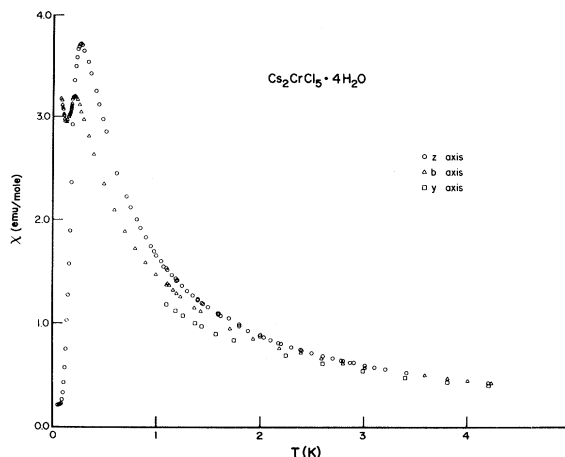


FIG. 3. Experimental zero-field magnetic susceptibility of $\text{Cs}_2\text{CrCl}_5 \cdot 4\text{H}_2\text{O}$ along the three principal axes as characterized above; \circ : easy (z) axis; \triangle : b axis; \square : hard (y) axis.

temperature of 0.185 ± 0.005 K is obtained from the maximum slope of both χ_z and χ_b . The ratio $T(\chi_{\max})/T_c = 1.5$ for χ_z . At the lowest temperatures, the data seem to be leveling off to a finite value. This is due to experimental error or crystal misorientation and is of no significance.

The b -axis susceptibility likewise reaches a maximum, falls slightly at lower temperatures and then increases at the lowest temperatures. We associate this general behavior with the fact that χ_b is a perpendicular susceptibility in the ordered state.

The high-temperature (1–4.2 K) measurements exhibit a slightly anisotropic g tensor. Assuming $S = \frac{3}{2}$, we find $g_z \sim g_b = 1.98 \pm 0.01$ and $g_y = 1.95 \pm 0.01$. These are values typically found for chromium by EPR measurements.¹⁰ Necessarily, any crystal-field splittings due to nonzero D and E terms have to be much smaller than 1 K; otherwise, we would expect to observe an effective spin $S = \frac{1}{2}$ behavior above 1 K.

Now, assume for the sake of argument that the exchange constant J is much larger than the zero-field splitting parameters D and E . This implies that one can analyze the data in terms of the isotropic Heisenberg model with $S = \frac{3}{2}$. The measured ratio $T(\chi_{\max})/T_c$ of 1.5 for χ_{\parallel} implies a lower-dimensional magnetic interaction in $\text{Cs}_2\text{CrCl}_5 \cdot 4\text{H}_2\text{O}$. If the material is behaving as a linear chain or one-dimensional antiferromagnet, the maximum value of χ_z of 3.71 emu/mol yields, using the results of de Jongh,¹³ the parameter zJ/k_B of value -0.072 K. But, from the temperature at which the maximum occurs, one calculates

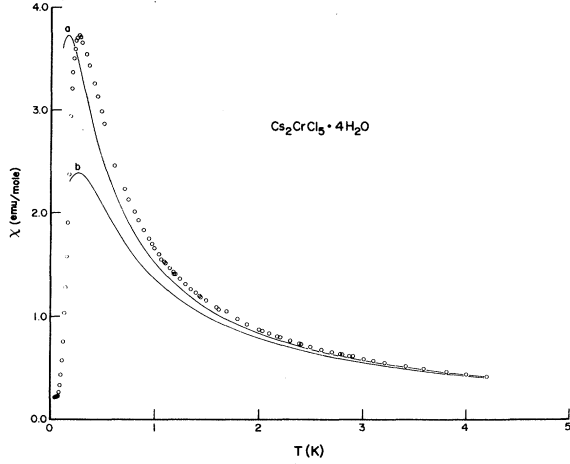


FIG. 4. Susceptibility χ_z and the curves corresponding to the linear-chain antiferromagnet that fit the experimental χ_{\max} value (curve *a*, $zJ/k_B = -0.072$ K), and the experimental T_{\max} (curve *b*, $zJ/k_B = -0.114$ K). In both cases, g is taken as 1.98.

$zJ/k_B = -0.114$ K. These calculations, obtained from Pade approximants to the high-temperature series¹⁴ (HTS) are compared with experiment in Fig. 4. Clearly these results are inconsistent with each other and with the experiment. On the other hand, assuming instead a two-dimensional quadratic lattice, for example, the value of $\chi(T_{\max})$ yields $zJ/k_B = -0.085$ K, while the value of T_{\max} yields¹³ $zJ/k_B = -0.137$ K. These values too are inconsistent with one another, and we therefore conclude that the above assumption that the crystal-field splittings are small compared to the exchange interactions is not tenable.

Since we are not aware of any HTS expansions for quantum-mechanical spin $S = \frac{3}{2}$ on chains with crystal-field anisotropies, we turn to the classical Eqs. (3)–(5), which are valid when D , E , and J are all smaller than $k_B T$. Plots of $\chi_i T$ vs $1/T$ are presented in Fig. 5, where it will be seen that straight lines are indeed obtained at high temperatures. Preliminary values of the parameters were obtained graphically and then were refined using the complete equations, Eqs. (1) and (2). We find the resulting parameters as

$$\begin{aligned} g_b = g_z &= 1.98 \pm 0.01, \\ g_y &= 1.95 \pm 0.01, \\ D/k_B &= -0.16 \text{ K} \pm 0.02, \\ E/k_B &= -0.05 \text{ K} \pm 0.01, \\ zJ/k_B &= -0.09 \text{ K} \pm 0.01, \end{aligned} \quad (7)$$

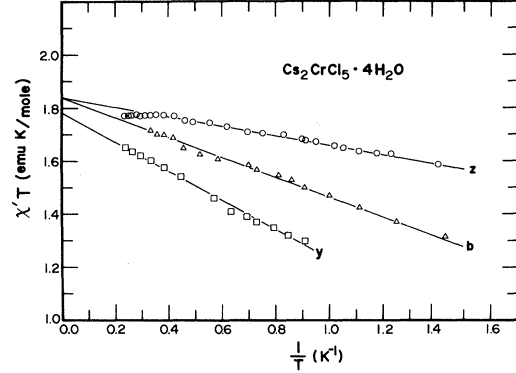


FIG. 5. Experimental susceptibility of $\text{Cs}_2\text{CrCl}_5 \cdot 4\text{H}_2\text{O}$ above 0.7 K plotted as $\chi_i T$ vs $1/T$. The linear least-squares fits to Eqs. (3)–(5) in the three principal directions provide the constants g_b , g_y , and g_z (from the ordinate intercepts), and D , E , and J (from the slopes).

or if linear-chain ($z=2$) behavior is assumed, $J/k_B = -0.045$ K.

As a test of the validity of this analysis, we have turned to Fisher's¹⁵ classical model for a one-dimensional system as modified by Smith and Friedberg¹⁶ for axial anisotropy. The relevant set of equations is

$$\chi_0 = \frac{Ng^2 S(S+1)\mu_B^2}{3k_B T} \left[\frac{1+\mu}{1-\mu} \right], \quad (8)$$

with

$$\mu = \coth[2JS(S+1)/k_B T] - \frac{k_B T}{[2JS(S+1)]}, \quad (9)$$

$$\chi_{\parallel} = \chi_0 - \left(\frac{4}{15}\right) \chi_c [DS(S+1)/k_B T] F, \quad (10)$$

$$\chi_{\perp} = \chi_0 + \left(\frac{2}{15}\right) \chi_c [DS(S+1)/k_B T] F, \quad (11)$$

where

$$\chi_c = Ng^2 \mu_B^2 S(S+1)/3k_B T, \quad (12)$$

and

$$F = \frac{(1+\mu)(1+v)}{(1-\mu)(1-v)} + \frac{2\mu}{(1-\mu)^2}, \quad (13)$$

with

$$v = 1 - [3\mu k_B T / 2JS(S+1)], \quad (14)$$

where all the terms have already been defined and we scale the theory to $S = \frac{3}{2}$. The analysis of the

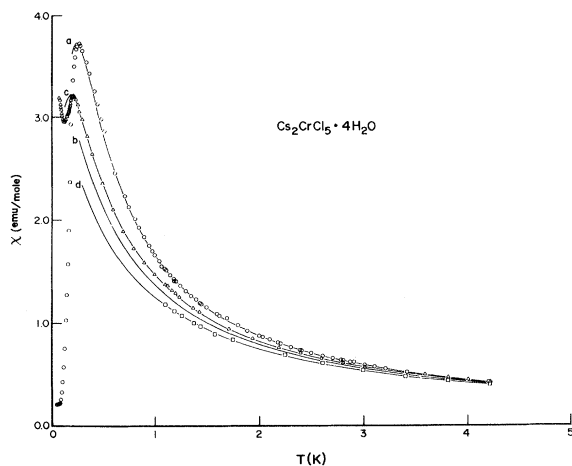


FIG. 6. Susceptibility of $\text{Cs}_2\text{CrCl}_5 \cdot 4\text{H}_2\text{O}$ along the three principal axes. Curves *a* and *b* represent the parallel and perpendicular susceptibility, respectively, for a classical one-dimensional system with axial anisotropy with $g=1.98$, $D/k_B=-0.16$ K, and $J/k_B=-0.0445$ K. Curves *c* and *d* are the fit for χ_b and χ_y , as explained in the text.

data in terms of Eqs. (10) and (11) is presented in Fig. 6. Curve *a* is associated with χ_{\parallel} , which is not affected by a rhombic distortion, and may be seen to fit very well. The parameters are $g=1.98$, $D/k_B=-0.16$ K, and $J/k_B=-0.0445$ K, which are in excellent agreement with the parameters presented above. The curve *b*, calculated with the same parameters, in Fig. 6 represents χ_{\perp} [Eq. (11)] and it will be seen to lie between the experimental values of χ_b and χ_y ; we attribute the lack of agreement to not having taken the rhombic term E into account.

To resolve this problem to a first approximation, looking at Eqs. (3)–(5), we expect that we can find χ_b in this model by substituting an effective parameter $D_{\text{eff}}=D-3E$, and χ_y by substituting $D+3E$ by D'_{eff} . From the parameter values, Eq. (7), we see that $D_{\text{eff}}=D-3E \sim 0$, and so we expect the linear-chain equation without any crystal-field term [i.e., an isotropic susceptibility, Eq. (8)] to fit the χ_b data, and this is represented by curve *c* in Fig. 6. The fit is indeed excellent. Furthermore, using the same parameter values to measure $D'_{\text{eff}}=D+3E$, we are able to fit the perpendicular susceptibility χ_y by Eq. (11) (curve *d*, Fig. 6). We note that the rhombic (E) term enters both Eqs. (3) and (4), with opposite sign, but not Eq. (5) at all. This is the reason why both D_{eff} and D'_{eff} must be used. Thus, the same set of parameters can be used to fit the data within either approximation.

DISCUSSION

The successful analysis of the susceptibility data of $\text{Cs}_2\text{CrCl}_5 \cdot 4\text{H}_2\text{O}$ has been carried out in terms of a Heisenberg linear-chain antiferromagnet. This is a model system which should undergo long-range order only at 0 K. Interaction between the chains as well as anisotropy lead to a finite transition temperature, and so the data analysis is valid only at temperatures high with respect to T_c . In practice, this means the analysis is valid down to approximately the temperature of the susceptibility maximum.

We have emphasized the linear-chain nature of this system because that follows directly from the earlier discussion of the likely superexchange paths. In retrospect, the successful data analysis in terms of the Heisenberg linear-chain model gives added credence to the validity of this application of this model to this system. A comparison of the data with HTS expansions for linear chains and quadratic lattices suggests to us that an analysis in terms of a planar rectangular lattice would improve the agreement between the experimental data and the theoretical fit, but that has been prevented by the lack of theoretical guidance for the behavior of a two-dimensional $S=\frac{3}{2}$ antiferromagnet. All the experimental data as well as the structure of $\text{Cs}_2\text{CrCl}_5 \cdot 4\text{H}_2\text{O}$ argue against the usual three-dimensional magnetic ordering.

Previous investigations of chromium(III) antiferromagnets fall largely into two classes. The first concerns such systems as CrCl_3 ($T_c \sim 16.8$ K), CrBr_3 ($T_c \sim 32$ K), and Cr_2O_3 ($T_c \sim 308$ K), all of which order at temperatures so high that the crystal-field splittings of the 4A_2 ground state have no effect on the magnetic ordering phenomena. The second concerns the alums, which order at such low temperatures (~ 10 mK) that dipole-dipole interaction is the main source of magnetic interaction. Because these systems are cubic, the crystal-field splittings have been determined primarily by EPR techniques. An earlier investigation² of $[\text{Cr}(\text{NH}_3)_6](\text{ClO}_4)_2\text{Br} \cdot \text{CsBr}$ showed that the zero-field splittings in this compound were much larger than the exchange interaction. The present report on $\text{Cs}_2\text{CrCl}_5 \cdot 4\text{H}_2\text{O}$ therefore appears to be the first example where crystal-field and exchange terms are of comparable magnitude and have been determined by susceptibility measurements alone. An independent measurement of the crystal-field terms by EPR would be desirable but we know of no isomorphous diamagnetic host which could serve as a suitable diluent.

The negative sign of the parameter D/k_B suggests that the $|\pm \frac{3}{2}\rangle$ state lies lowest. If D/k_B were much larger than J/k_B , then one would anticipate Ising magnetic ordering as for example with Cs_3CoCl_5 (Ref. 17); one consequence of this is that much larger anisotropy would be expected to be found in the susceptibilities than is observed. Thus, in agreement with the analysis presented, the crystal-field terms are neither much larger than nor much smaller than the exchange interaction. The method of analysis can best be described as approximate, for there are not available any complete calculations of the susceptibilities for an $S = \frac{3}{2}$ linear-chain magnet with crystal-field terms.

Green $\text{CrCl}_3 \cdot 6\text{H}_2\text{O}$ also contains the *trans*- $[\text{CrCl}_2(\text{H}_2\text{O})_4]^+$ chromophore. We have measured the susceptibility of a polycrystalline sample of this

material over the temperature interval 1.2–4.2 K, and find the data obey the Curie-Weiss law quite well, with $\langle g \rangle = 1.978 \pm 0.005$ and $\Theta = -0.13 \pm 0.02$ K. These parameters are quite typical for a chromium(III) compound. The compound is hygroscopic and forms poor crystals, so it was decided not to measure the susceptibility at lower temperatures.

ACKNOWLEDGMENT

This research was supported by the Solid State Chemistry Program, Division of Materials Research of the National Science Foundation, through Grant No. DMR7906119. We thank A. Pilipowicz for the preparation of the sample and his assistance.

-
- ¹R. L. Carlin, *J. Appl. Phys.* **52**, 1993 (1981).
²R. D. Chirico and R. L. Carlin, *Inorg. Chem.* **19**, 3031 (1980).
³B. E. Myers, L. G. Polgar, and S. A. Friedberg, *Phys. Rev. B* **6**, 3488 (1972).
⁴J. N. McElearney, D. B. Losee, S. Merchant, and R. L. Carlin, *Phys. Rev. B* **7**, 3314 (1973).
⁵R. L. Carlin, C. J. O'Connor, and S. N. Bhatia, *J. Amer. Chem. Soc.* **98**, 3523 (1976).
⁶H. A. Algra, L. J. de Jongh, and R. L. Carlin, *Physica B* **92**, 258 (1977).
⁷J. A. Puertolas, R. Navarro, F. Palacio, J. Bartolome, D. Gonzalez, and R. L. Carlin, *Phys. Rev. B* **26**, 395 (1982), and references therein.
⁸P. J. McCarthy, J. C. Lauffenburger, P. M. Skonezny, and D. C. Rohrer, *Inorg. Chem.* **20**, 1566 (1981).
⁹A. van der Bilt, K. O. Joung, R. L. Carlin, and L. J. de Jongh, *Phys. Rev. B* **22**, 1259 (1980).
¹⁰B. R. McGarvey, in *Transition Metal Chemistry*, edited by R. L. Carlin (Dekker, New York, 1966), Vol. 3, p. 130.
¹¹P. Ganguli, V. R. Marathe, S. Mitra, and R. L. Martin, *Chem. Phys. Lett.* **26**, 529 (1974).
¹²J. N. McElearney, S. Merchant, and R. L. Carlin, *Inorg. Chem.* **12**, 906 (1973).
¹³L. J. de Jongh and A. R. Miedema, *Adv. Phys.* **23**, 1 (1974).
¹⁴G. S. Rushbrooke and P. J. Wood, *Mol. Phys.* **1**, 257 (1958).
¹⁵M. E. Fisher, *Am. J. Phys.* **32**, 343 (1964).
¹⁶T. Smith and S. A. Friedberg, *Phys. Rev.* **176**, 660 (1968).
¹⁷H. W. J. Blöte and W. J. Huiskamp, *Phys. Lett. A* **29**, 304 (1969).